Pilot-scale investigation of two Electric Pulse Fragmentation (EPF) approaches for the mineral processing of a low-grade cassiterite schist ore

Kathy Bru[a,*], Rui Sousa[b], Mário Machado Leite[b], Chris Broadbent[c], Garfield Stuart[c], Dzmitry Pashkevich[d], Mirko Martin[d], Marius Kern[e], Daniel B. Parvaz[f]

[a] BRGM, F-45060 Orléans, France
[b] LNEG National Laboratory of Energy and Geology, S. Mamede de Infesta, Portugal
[c] Wardell Armstrong International, Wheal Jane Earth Science Park, Baldhu, Truro, Cornwall TR3 6EH, UK
[d] GEOS, Gewerbepark Schwarze Kiefern 2, 09633 Halsbrücke, Germany
[e] Helmholtz-Zentrum Dresden-Rossendorf, Helmholtz Institute Freiberg for Resource Technology, Chemnitzer Straße 40, 09599 Freiberg, Germany
[f] SELFRAG AG, Biberenzelgli 18, 3210 Kerzers, Switzerland

ARTICLE INFO

ABSTRACT

Two approaches for the use of the Electric Pulse Fragmentation (EPF) in the beneficiation of a low-grade cassiterite schist ore were investigated through pilot-scale tests performed on samples of about 270 kg. The first approach used EPF treatment for pre-concentration while in the second approach the EPF technology was mostly used for crushing. Comparison with the use of conventional crushers was performed.

Results showed that the EPF pre-treatment led to a decrease of the Bond rod mill work index while the Bond ball mill work index remained unchanged. This means that the decrease in the energy consumption requested to grind the material down to 1.18 mm (closing screen of the Bond rod mill work index) is no longer noticeable with additional grinding stage to reach a size down to 106 μm (closing screen of the Bond ball mill work index). This may be due to the fracture network generated during EPF being consumed immediately in the subsequent comminution step. Alternatively, it may be that the Bond ball mill work index is not appropriate for exhibiting the weakening effect of the EPF technology when the mineral liberation size is coarser than the closing screen size used for the test. Concentration tests performed on the sample treated with the first approach for EPF showed no marked change in separation performance. However, a higher concentrate grade was obtained when using this EPF pre-treatment, indicating a probable potential for improvement.

1. Introduction

Tin is used in a wide range of applications due to its malleability, ductility and resistance to corrosion. In particular, these applications include metal coating, tin plating, alloying, soldering, and plumbing (Angadi et al., 2015). The demand for these properties in the electronic and electrical industries makes it a vital ingredient in a wide range of manufacturing sectors, including consumer goods, packaging, construction, vehicles and other forms of transport (ITA, 2013). As a result, tin consumption is expected to rise dramatically in the coming years due to newly developed end uses, including as an advanced anode material in Li ion batteries (Kamali and Fray, 2011; Sultana et al., 2016).

The minerals industry in general is facing the dual problems of increasing ore competence with declining overall grades, meaning higher volumes of harder rock must be processed each year to recover the same amount of metal, resulting in increased overall energy consumption. One potential solution to the problem of excessive energy usage is to reject gangue rock from a material flow at an early stage, thereby expending less energy in the comminution of waste. Coarse rejection of waste upgrades the ore by concentrating the valuable minerals, and in the case of competent gangue, such as highly silicified rocks, this can also improve the grindability of the material. This pre-concentration (Zuo et al., 2015) potentially allows reduced energy usage and increased recovery, a step-change in mineral processing circuits (Bearman, 2013).

Cassiterite is the primary economic tin mineral. It is heavy (specific gravity = 6.9-7.1), hard, extremely brittle in nature and is generally associated with lighter gangue minerals. Cassiterite occurs both in deep hard rock mines and near surface alluvial deposits (ITA, 2013). Alluvial
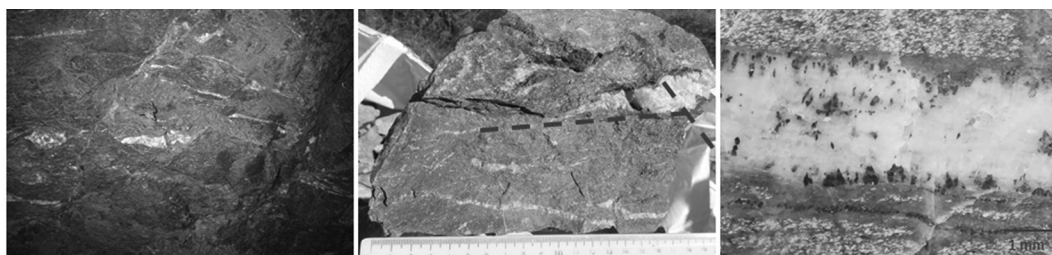
---

* Corresponding author.
  E-mail address: k.bru@brgm.fr (K. Bru).

Fig. 1. Schist ore sampling wall, specimen collected after blasting with flat lying quartz veinlets, microscopic view of cassiterite growth from the vein walls towards the center (from left to right respectively).

deposits are easy to beneficiate using gravity units due to the coarse liberation size (Moncrieff and Lewis, 1977), while hard-rock cassiterite is often associated within a granite and is harder to beneficiate due to fine liberation size (Angadi et al., 2015), requiring various steps of comminution, classification, gravity concentration and flotation. Cassiterite's brittle nature means that careful design of the processing flowsheet is required to avoid overgrinding and loss of cassiterite to tailings. Most of the recent works performed on cassiterite processing is related to the enhanced gravity concentrations and flotation in order to improve the recovery of the cassiterite found in the fine fraction (Angadi et al., 2015).

Another approach for improving cassiterite recovery and reducing energy expenditure in comminution is to implement a selective comminution technology, which has the advantage of reducing fines production by generating cracks specifically at the boundaries between mineral grains rather than randomly as in a conventional mechanical comminution system. This allows the liberation of valuable components from the feed material without overgrinding. Liberation at coarser size ranges is not only beneficial for the subsequent separation techniques, but can also lead to significant economic benefits for mineral processing operations such as a reduction in the grinding energy since the material does not need to be ground as finely as in conventional comminution systems (Wang et al., 2012). In addition, the rocks which are not fragmented by the process are usually weakened by the dense fracture network generated, which increases grindability of the material (Wang et al., 2011). Selective comminution technologies that specifically target metallic phases of an ore have been shown to preferentially concentrate metal-bearing minerals into the finer product, while gangue remains coarse (Zuo et al., 2015; Shi et al., 2015).

Selective comminution methods are usually based on anisotropic properties of the ore and related to varying properties of constituent minerals (e.g. mechanical, electrical or acoustic properties, thermal expansion). Electric Pulse Fragmentation (EPF) is one such technique that exploits differences in electrical and acoustic properties of a material's component phases to selectively fragment it. EPF works by applying highly energetic electrical pulses (150–750 J/pulse) with a very fast pulse rise time (< 500 ns) to materials immersed in a dielectric process liquid (usually water). Dielectric liquids such as water are more resistive than solids at this pulse rise time, forcing discharges through the immersed material. Upon discharge, a plasma channel forms that causes explosive expansion along its pathway through the material, and the collapse of the plasma channel produces a shock wave that propagates through the material (electrodynamic fragmentation). The high selectivity of the process arises from the way the electricity and shockwaves interact with physico-chemical properties of the material: discontinuities in mineral-specific electrical permittivity and conductivity at phase boundaries locally enhance the electric field forcing the discharge streamers to these boundaries and increasing the likelihood of discharge along these grain boundaries. The combination of the shock wave with acoustic discontinuities concentrates tensile stress at phase interfaces (Andres et al., 1999) causing breakage at these boundaries, allowing full liberation of components from the feed material. The potential of this technique to improve liberation and

grindability of ores was already demonstrated by several authors (Andres et al., 1999; Wang et al., 2012; Shi et al., 2013; Bru et al., 2018) but its application to a schist ore with a low cassiterite grade has not yet been reported.

This work aims to investigate the influence of two EPF approaches for the mineral processing of a low-grade schist ore containing cassiterite. The first approach consists in using the EPF treatment for pre-concentration while in the second approach the EPF technology is mostly used for crushing, improvement in the mineral liberation being expected in both approaches. EPF was performed at pilot-scale to better simulate industrial processing conditions, and to have the opportunity to investigate the influence of this treatment on the downstream concentration processes.

2. Materials and methods

2.1. Ore samples

The ore used in this study is a tin schist ore from the Hämmerlein deposit located in the Erzgebirge in Germany. The Hämmerlein deposit is a polymetallic deposit that comprises a Sn-In-Zn skarn and a greisenized shale called Schiefererz (Schuppan and Hiller, 2012). Schist in Hämmerlein is fine-to-medium grained (< 0.5 mm) and predominantly consists of quartz and mica (muscovite and biotite) with variable amounts of feldspars (mainly K-feldspar and Na-plagioclases). The cassiterite (SnO_2) mineralization precipitated in veinlets of 0.5–15 mm thickness together with chlorite, fluorite, rutile, tourmaline, and quartz forming schist ore, as shown in Fig. 1. The mineralization is greisen-style with developed stockwork and flat lying foliation. Schist ore mineralized with tin is most commonly located in the footwall of the skarn but can sometimes also be found in the hanging wall. The schist ore head grade for Sn is about 1.1 wt% (determined by XRF). The major elemental composition obtained from ICP analysis is 72.6% SiO_2, 12.8% Al_2O_3, 3.4% K_2O, 1.4% MgO, 0.8% CaO, 0.8% Na_2O and 0.6% TiO_2. The ore also contains 5.1% Fe_2O_3, 109 ppm Cu, 100 ppm S, 79 ppm Zn, 73 ppm W and 19 ppm As.

According to deportment calculations from Mineral Liberation Analysis (MLA), more than 99 wt% of tin in the sample derives from cassiterite which is primarily associated to quartz (31%) and mica (37%) (Fig. 2). Morphologically, cassiterite grains are predominantly subhedral to euhedral. Its mean diameter is about 161 μm but particles as small as 10 μm can also be found. It should be mentioned that MLA was performed on a sample crushed down to 630 μm and classified into 3 fractions (< 100 μm, 100/250 μm and 250/630 μm) for preventing bias related to settling, as indicated by Heinig et al. (2015).

This ore has a crushability of about 19.1 kWh/t (measured with a Bond low energy impact test) and a Bond work index of 16.1 kWh/t.

The samples were collected 2400 m from the main adit (Stolln Pöhla) entrance of Hämmerlein mine at the level +590 m (Fig. 3). Two samples were collected at the same location, but at a different date. The sample from the first sampling campaign was used for testing the conventional route and the sample from the second campaign was used for investigating the influence of the EPF technology in the
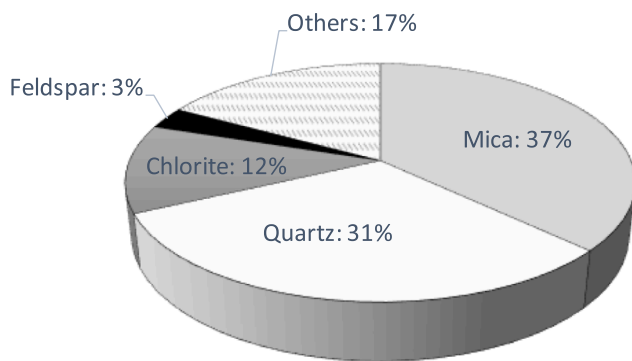
Fig. 2. Structure of mineral associations for cassiterite in a schist sample crushed below 630 μm (liberated cassiterite grains are not considered) based on Mineral Liberation Analysis results.

beneficiation flowsheet. The particle size distribution of these 2 samples is given in Fig. 4. A similar Sn grade was observed for these two samples with a grade of 1.18% for the sample collected during the first sampling campaign and 1.27% for the one collected during the second campaign. The two samples have also a close abrasion index, being 0.3439 and 0.2182 for the sample collected during the first and the second campaign respectively. These similarities, combined with the fact that the two samples were collected at the same location in the mine, allowed performing reliable comparison of the results obtained with the conventional and with the EPF pathway.

3. Experimental set-up

3.1. EPF pilot-scale test

Tests were performed with the SELFRAG Scoria pilot plant (Fig. 5, Fig. 6) which is designed for the continuous high voltage fragmentation of bulky materials. The modular pilot plant is comprised of a single

SELFRAG 'Explorer' generator above a 'Scoria' process zone (PZ) into which discharges occur. The generator steps the mains 400 V up to between 90 and 190 kV, and is capable of delivering 3.75 kW per hour to the PZ, and therefore to the material to be processed. A full list of system variables is presented in Table 1. The Scoria PZ is designed for the transport and processing of material 2/50 mm in size, with a throughput of several t/h depending on specific energy input and material specific gravity. A feed-in vibrating chute transports material into the PZ which incorporates a conveyor that draws it between the electrodes where it receives an amount of energy proportional to the residence time. Fragmented material is then removed from the PZ by the conveyor for collection in a container, or for further material transport and separation. Energy discharged to the sample is determined by calculating the joules per electrical pulse (JPP), a function of system voltage and capacitance, then multiplying JPP by the total number of discharges recorded by the system when all material is processed. This total energy input is then divided by the mass of material to give a discharged energy value in kWh/t. More information on the calculation of the JPP can be found in Zuo (2015).

Two approaches for the EPF treatment were implemented during this campaign:

- The first approach (Test 1) was performed with the objective of assessing if the EPF technology could be considered as a pre-concentration step. One EPF treatment step of the material was performed at a discharged energy of 6.5 kWh/t, this discharged energy being chosen based on previous works performed at lab scale.
- The second approach (Test 2) used the EPF system as a crushing equipment. After a first EPF treatment step performed at a discharged energy of about 6.5 kWh/t, the products were sieved at 5 mm and the oversize was reprocessed in the EPF plant at the same discharged energy. This was repeated twice and then the oversize and the undersize were combined. The overall discharged energy was evaluated to 12.5 kWh/t.

Tests were performed on a sample of about 540 kg previously
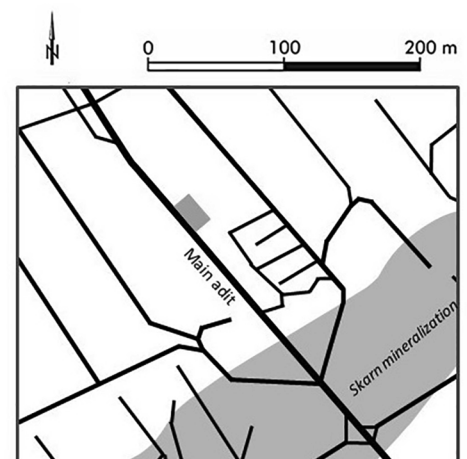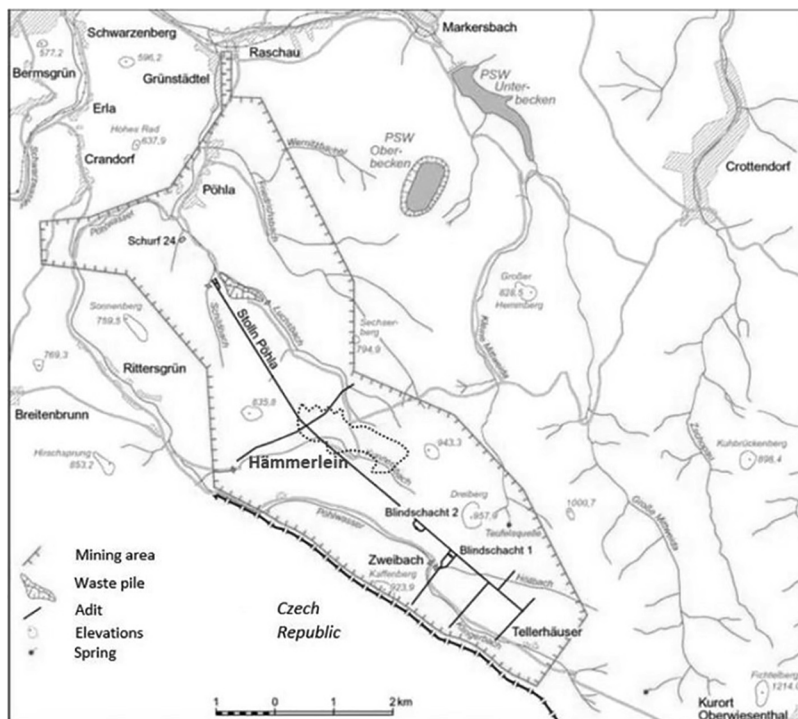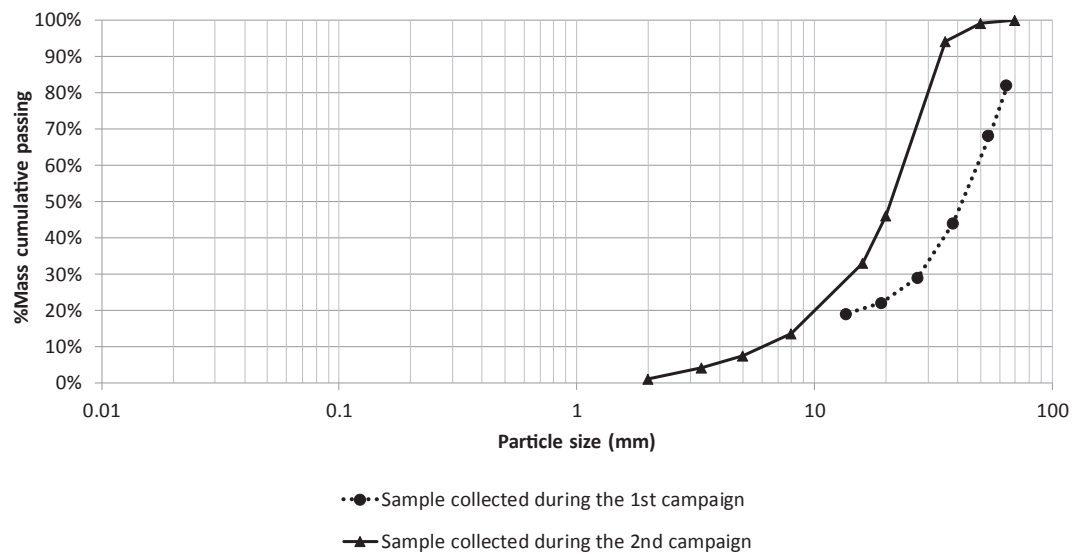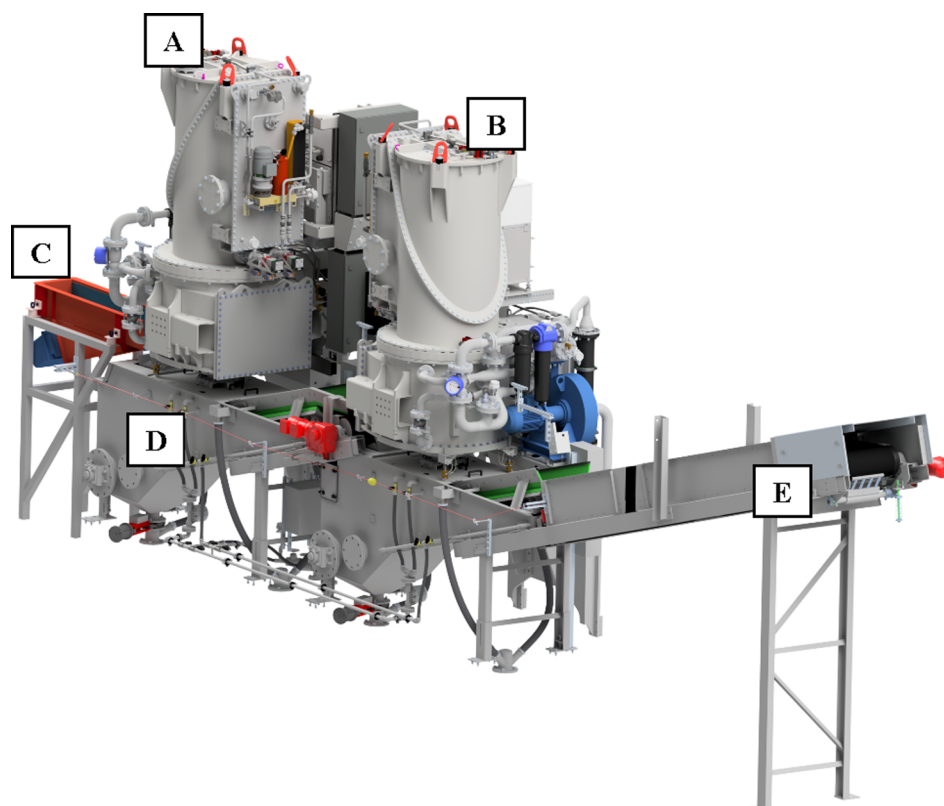

Fig. 3. Sampling location in the Hämmerlein deposit during the first and the second sampling campaigns (left image modified after Schuppan and Hiller (2012), grey box on the right image modified after Kern et al. (2018)).

Fig. 4. Particle size distribution of the samples collected from the first and the second collecting campaign.

crushed at 50 mm and sieved at 2 mm in order to remove particles which are too fine for feeding into the EPF machine. This sample was then divided into two representative samples of about 270 kg for the two EPF tests.

3.2. Concentration tests

Concentration tests were performed with a Mozley Laboratory Separator (MLS) to assess the effect of EPF pre-treatment on the cassiterite upgrading stage. For this purpose, a sample collected in the first sampling campaign was primarily crushed in a jaw crusher followed by a cone crusher and then by a roll crusher to reduce all material below 850 µm. A circular screen was used for size classification. A similar procedure was applied to a sub-sample of the product of EPF Test 1, except that this sample was directly fed into the cone crusher.

Then, two standard trays were used depending on the size fraction to process: the "Flat" profile tray was used to test the size fraction < 75 µm and the "V" profile tray was used to test the size fractions coarser than 75 µm (75/212 µm, 212/425 µm and 425/850 µm). Fig. 7 shows the procedure and sample collection. For each test performed on each size fraction, five products were collected: tailings; low-grade middlings; middlings; high-grade middlings; and concentrate.

3.3. Characterization method

The particle size distribution (PSD) was measured by manual sieving at thirteen sizes (40 mm, 31.5 mm, 20 mm, 16 mm, 8 mm, 5 mm, 3.36 mm, 2 mm, 1 mm, 500 µm, 250 µm, 125 µm and 63 µm), which enabled estimation of the product sizes P80 and P50 (i.e. 80% passing size and 50% passing size respectively).

Fig. 5. SELFRAG Scoria pilot plant featuring Explorer Generator incorporating: A: Explorer Generator; B: Feed in conveyor; C: Process Zone with electrode head; D: Feed out conveyor.

Fig. 6. CAD Render of Scoria plant incorporating 2 generators. A: Generator 1; B: Generator 2; C: Feed in vibrating plate; D: Process zone with inbuilt conveyors; E: Feed out conveyor (from Parvaz et al., 2019).

Table 1
Scoria (explorer) plant equipment settings and ranges.

Equipment variable	Range
Distance between electrodes (electrode gap)	30–50 mm
Voltage (pulse power)	90–200 kV
Pulse repetition rate (frequency)	1–5 Hz
Conveyor speed	0–1000 mm/s

The Sn content was determined by a portable X-Ray Fluorescence analyzer in the section related to the characterization of the products obtained after the two EPF tests. Representative splits of each sample were pulverized before analysis and calibrated against in-house Sn standards. In the section related to concentration tests, the Sn content was measured by WDS - X-Ray Fluorescence spectrometry (Philips – PW 2404 X-ray Spectrometer).

Regarding physical testing, the following tests were performed: abrasion index, Bond rod mill work index (with a closing screen size of 1.18 mm) and Bond ball mill work index (with a closing screen size of 106 μm).

4. Results and discussion

4.1. Characterization of the products obtained after the two EPF tests

The PSD of the products obtained after the two EPF tests is given in Fig. 8 and the related products sizes P80 and P50 are reported in Table 2. A strong reduction in particle size after the 6.5 kWh/t test (Test 1) is observed. Increasing the discharged energy input from 6.5 to 12.5 kWh/t led to a reduction in product size (Test 2), however overall product size reduction was not linearly correlated with energy input: multiplying the energy input by a factor 1.9 (from 6.5 to 12.5 kWh/t)

only led to a reduction in P80 by a factor 1.4 (from 15.0 to 11.0 mm). This is due to the non-linear relationship between energy input and size reduction as already observed by several authors (van der Wielen et al., 2013; Zuo et al., 2015; Bru et al., 2018). Fig. 8 also shows the PSD of the products obtained after a conventional crushing performed with a jaw crusher down to 20 mm. Results show that the conventional crushing led to coarser product. However, when comparing not the whole particle size range but only particles smaller than 1 mm (Fig. 9), it can be observed that conventional crushing led to the production of a higher amount of fine particles compared to the EPF technology, as already observed by Tschugg and al. (2017).

Fig. 10 shows the Sn grade for each size fraction after both conventional crushing and EPF as described in the Section 2.2 of the Materials and Methods. There is an increase in the Sn grade in the fractions lower than 1 mm for the two EPF tests combined with a slight depletion in the coarsest fractions (Fig. 10). This can be explained by the fact that as EPF treatment selectively fragments the rock, metal-rich particles are preferentially broken away from the host rock while gangue remains coarse (Zuo et al., 2015) resulting in metal deportment to the undersize for a given sieve cut. Results show that the Sn grade is very similar in all size fractions of the product obtained after conventional crushing, confirming then the selectivity of EPF.

To compare the performances of the EPF approaches the cumulative Sn distribution from fine to coarse sizes was plotted to show the effectiveness of a selective screening applied after comminution (Fig. 11). The diagonal line in Fig. 11 represents the results of a random comminution; it is called "No-upgrading line" (after a selective screening) since in a random comminution each size class will have the same grade, which will be similar to the ore average grade. The distance between the EPF Sn distribution and the no-upgrading line gives an indication of the upgrading degree of the ore. An improvement in the Sn distribution is observed with the two EPF tests, but this improvement is limited, indicating that EPF treatment provided only a small 'pre-
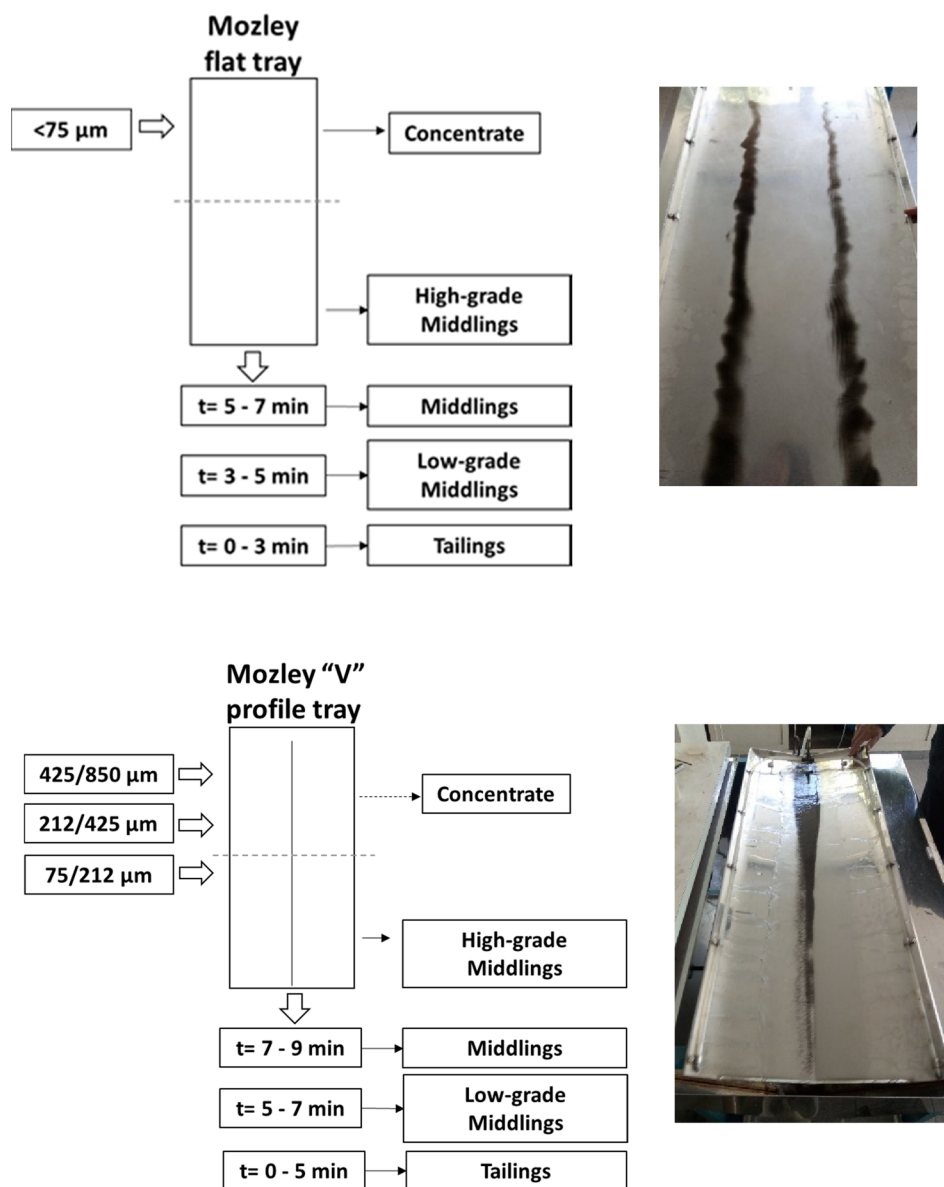
Fig. 7. Experimental procedure and sample collection for the tests with the Mozley Laboratory Separator.

concentration' effect. This may be due to the very low cassiterite content of the ore, meaning a greater number of discharges interacting with gangue, dampening the pre-concentration effect.

Results from physical testing are given in Table 3 and shows an strong increase in the abrasion index of the products obtained after the two EPF tests. As the abrasion index is measured on the size fraction 12.5/20 mm, an hypothesis could be that EPF led to an increase in the coarse fraction of the content of some abrasive gangue particles such as quartz due to preferential crushing of metal enriched particles and coarse liberation of gangue. An increase in the abrasion index has not been observed before. More tests are then required to determine the cause of the increase in the abrasion index, if it is due to the EPF treatment or another factor. Considering its importance for the operation of a comminution plant, this result show that it is essential to perform abrasion index measurement when studying the potential of the EPF technology.

A reduction in the Bond rod mill work index (Table 3) is observed after EPF treatment, thus confirming the weakening effect of the EPF treatment on this sample. A Bond rod mill work index of 16.32 kWh/t was measured for the sample before treatment, while values of 13.89

kWh/t for Test 1, and 12.89 kWh/t for Test 2 were obtained after treatment, which corresponds to a grinding energy reduction of 14.9% and 21.0% respectively. This improvement of the grindability with the EPF treatment is no longer noticeable however when performing the Bond ball mill work index (Table 3). This corresponds with Tschugg et al (2017), which showed that EPF treatment can result in energy savings in the comminution step directly after EPF, however did not observe additional energy savings subsequently in the comminution flow sheet, most likely due to the fracture network generated during EPF being consumed immediately in the next comminution step. Another explanation for these results is material specific, in that the Bond ball mill work index is not appropriate for exhibiting the weakening effect of the EPF technology when the major gangue mineral liberation size is coarser than the closing screen size used for the Bond ball mill test (usually around 100 μm). When liberation size is sufficiently large, the feed will be composed of more resistant monomineralic particles such as quartz. Here, the mean liberation size was estimated to be from 156 to 467 μm for quartz and to 175 μm for cassiterite, while the closing screen size used for measuring the Bond ball mill work index was 106 μm. For this reason, the Bond work index tests should be
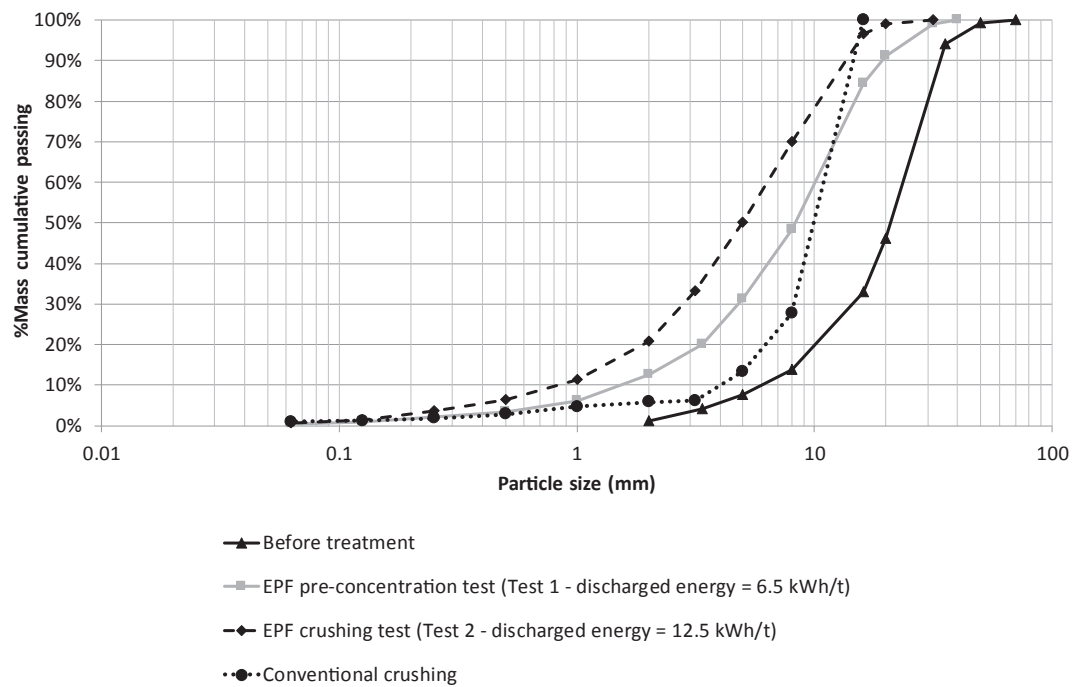
Fig. 8. Particle size distribution of the schist sample before EPF treatment and of the fragments after the two EPF tests and after a conventional crushing.

Table 2
Product sizes P80 and P50 of the schist samples before treatment, after the EPF treatments and after a conventional crushing.

	P80 (mm)	P50 (mm)
Schist ore before treatment	31.0	21.3
Sample after EPF pre-concentration test	15.0	8.4
(Test 1 – discharged energy: 6.5 kWh/t)		
Sample after EPF crushing test	11.0	5.0
(Test 2 – discharged energy: 12.5 kWh/t)		
Conventional crushing	13.8	10.5

coupled with mineral liberation analysis to give a better understanding of the results.

As such, the Bond rod mill work index, with a closing screen size of 1.18 mm, appears more relevant for studying the grindability of this ore and identifying any weakening effect of the EPF treatment. The energy consumption of the comminution circuit from coarse fragmentation to rod milling, i.e. taking into account the energy used for the first fragmentation step (either with conventional or with the EPF method), is given in Table 4 with the energy consumption of the jaw crushing steps implemented in the conventional pathway instead of the EPF treatment
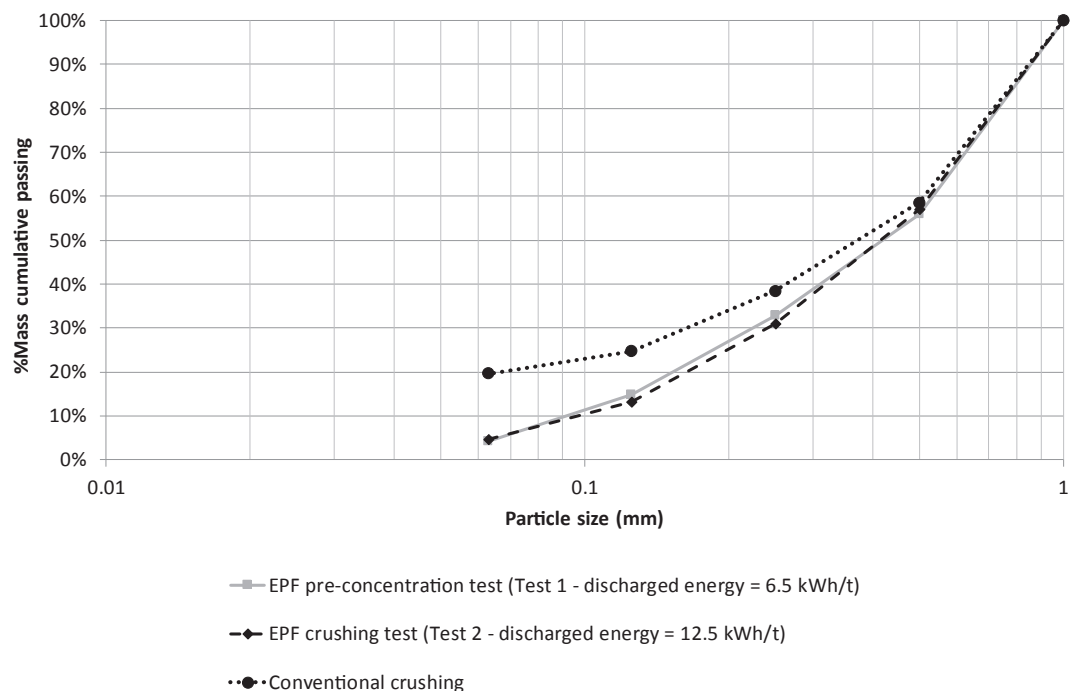

Fig. 9. Particle size distribution for the observation range 0–1 mm of the fragments after the two EPF tests and after a conventional crushing.
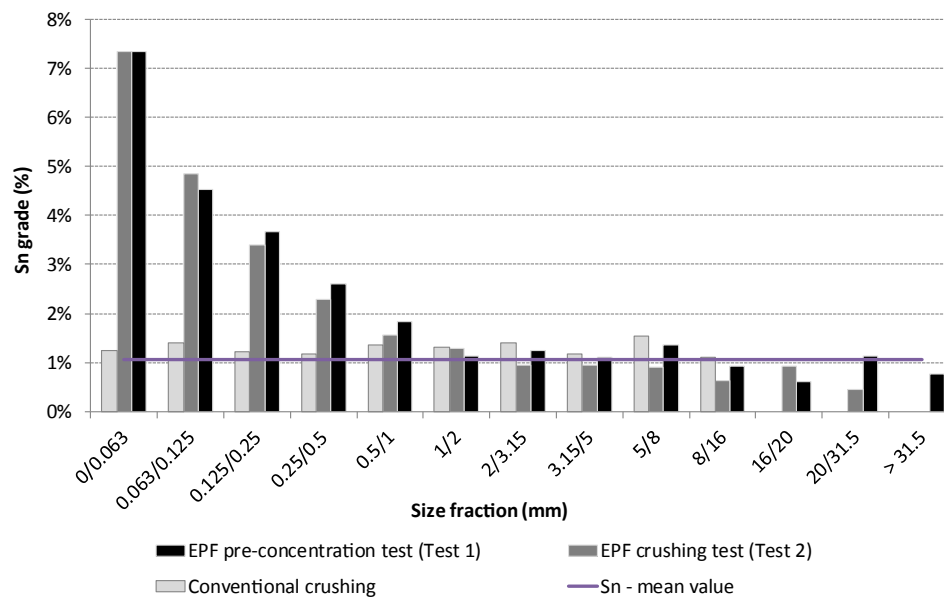
Fig. 10. Sn grade in each size fraction after the two EPF tests and after conventional crushing.
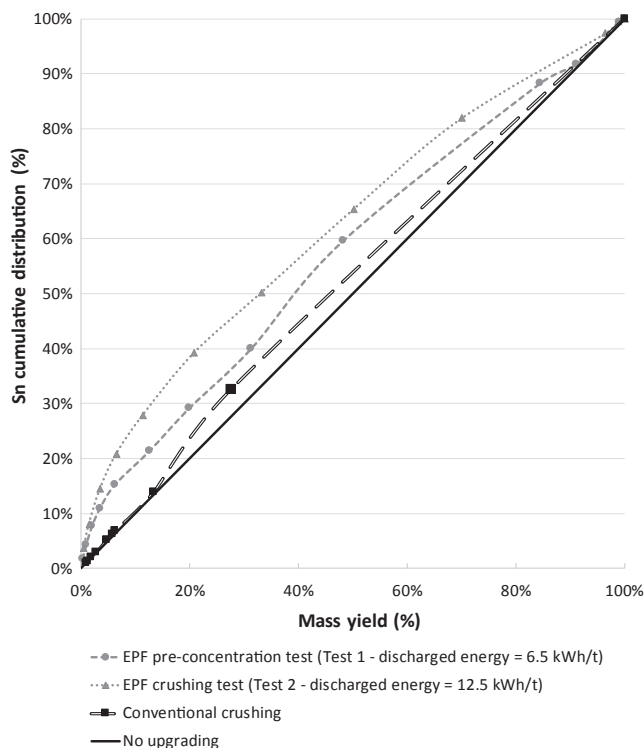

Fig. 11. Sn cumulative distribution after the two EPF tests and after conventional crushing.

estimated using the Bond formula law and the crushability index of the ore. Table 4 shows that using an EPF treatment in the comminution circuit leads to an increase of the overall comminution energy compared to the conventional route. This comparison should be considered carefully, however, since the discharged energy value of 6.5 kWh/t was chosen based on previous tests performed at lab-scale, and it was shown that the energy consumption of a batch lab-scale EPF equipment exceeds the one of a continuous pilot-scale EPF system for similar performances (Bru et al., 2018). It could therefore be possible that an EPF treatment performed at a discharged energy lower than 6.5 kWh/t still induces a marked weakening of the sample leading to a lower energy consumption of the whole comminution circuit.

4.2. Concentration tests

Concentration tests were conducted with a Mozley Laboratory Separator on conventionally crushed and EPF pre-treated (from Test 1) samples, both ground at 850 μm. The particle size distribution and the Sn grade of each size fraction of these 2 samples are given in Table 5. It can be observed that the sample from the conventional pathway is slighty finer than the one previously treated with the EPF technology with a P80 of 481 μm against 535 μm for the EPF pre-treated sample. An increase of the Sn grade in the coarsest size fraction (425/850 μm) was also observed for the sample previously treated with the EPF technology (1.45% in the whole sample vs 1.71% in the size fraction 425/850 μm), but this result should be considered carefully since the average head grade was slightly higher in the EPF-treated sample compared to the one of the sample used for the conventional pathway (1.45 %Sn and 1.32 %Sn respectively).

After the concentration test, it was observed that while EPF pre-treated sample led to higher concentrate grades in all size fractions, lower recoveries were achieved (Table 6). To assess the performance of

Table 3

Results related to the abrasion index, the Bond rod mill work index and the Bond ball mill work index of the schist samples before and after EPF treatment.

	Abrasion index	Bond rod mill work index (kWh/t)	Bond ball mill work index (kWh/t)
Schist ore before treatment*	0.3439	16.32	16.12
Sample after EPF pre-concentration test (Test 1 – discharged energy: 6.5 kWh/t)	1.1213	13.89	15.15
Sample after EPF crushing test (Test 2 – discharged energy: 12.5 kWh/t)	1.0736	12.89	16.33

* For the schist ore before treatment, physical testing were performed on a sample collected during the first sampling campaign.

Table 4

Energy consumption of the comminution steps from coarse fragmentation to rod milling for the two EPF routes and for a conventional pathway.

	Energy consumption (kWh/t)		
	Coarse fragmentation	Rod milling	Total
EPF Test 1 (pre-concentration test – discharged energy: 6.5 kWh/t)	6.5	13.9	20.4
EPF Test 2 (crushing test – discharged energy: 12.5 kWh/t)	12.5	12.9	25.4
Conventional treatment (the energy consumption of the crushing steps for coarse fragmentation was estimated to 0.7 kWh/t using the Bond formula law and the crushability index of the ore measured to 19.1 kWh/t)	0.7	16.3	17.0

Table 5

Particle size distribution and Sn grade of the samples used for the Mozley table tests.

		Technology implemented for the first fragmentation step			
		Conventional pathway (jaw crushers)		EPF Test 1	
		%mass cumul.	%Sn	%mass cumul.	%Sn
Size class	425/850 µm	100.00%	1.21	100.00%	1.71
	212/425 µm	76.95%	1.45	73.03%	1.30
	75/212 µm	58.93%	1.53	48.13%	1.68
	< 75 µm	30.30%	1.13	27.03%	1.15
	Total		1.32		1.45

Table 6

Results of release analysis from concentration tests performed with a Mozley Laboratory Separator.

		Technology implemented for the first fragmentation step					
		Conventional pathway			EPF pre-treatment (Test 1)		
		%mass	Sn		%mass	Sn	
			Grade %	Dist %		Grade %	Dist %
425/850 µm	Concentrate	4.78	13.09	51.66	4.36	15.08	38.44
	High grade middlings	16.12	0.93	12.42	4.38	6.31	16.13
	Middlings	24.00	0.81	16.12	30.37	0.97	17.21
	Low grade middlings	29.40	0.54	13.00	35.78	0.73	15.33
	Tailings	25.70	0.32	6.80	25.10	0.88	12.87
	Feed		1.21			1.71	
212/425 µm	Concentrate	7.25	13.89	69.45	2.77	31.30	66.64
	High grade middlings	39.78	0.62	17.02	12.62	1.16	11.23
	Middlings	31.44	0.44	9.44	57.30	0.39	17.15
	Low grade middlings	14.35	0.31	3.02	19.46	0.27	4.02
	Tailings	7.18	0.22	1.07	7.86	0.16	0.95
	Feed		1.45			1.30	
75/212 µm	Concentrate	4.20	30.51	83.43	1.59	73.30	69.24
	High grade middlings	10.43	0.92	6.25	4.46	8.00	21.20
	Middlings	30.94	0.21	4.19	28.55	0.28	4.67
	Low grade middlings	32.70	0.15	3.28	42.60	0.15	3.67
	Tailings	21.73	0.20	2.85	22.81	0.09	1.22
	Feed		1.53			1.68	
< 75 µm	Concentrate	1.50	50.00	66.85	1.15	67.20	67.54
	High grade middlings	2.95	3.74	9.80	11.04	1.61	15.53
	Middlings	13.82	0.51	6.23	46.05	0.17	6.96
	Low grade middlings	12.60	0.17	1.89	13.99	0.21	2.60
	Tailings	69.12	0.25	15.23	27.77	0.30	7.37
	Feed		1.13			1.15	
Overall	Concentrate	4.07	22.63	69.66	2.51	33.75	58.49
	High grade middlings	14.76	0.95	10.60	8.25	2.84	16.15
	Middlings	24.24	0.45	8.28	40.93	0.42	11.94
	Low grade middlings	22.54	0.29	4.93	27.27	0.38	7.23
	Tailings	34.38	0.25	6.53	21.05	0.43	6.18
	Feed		1.32			1.45	

mineral separation, an adequate method is to compute the efficiency curves. In this case, Mayer Diagrams (Fig. 12) were selected to compare the separation efficiency of both samples. Table 6 and Fig. 12 shows that:

– In the size fraction 425/850 µm, the concentration test performed

on the EPF pre-treated sample led to a slightly higher-grade concentrate. This can be due to a higher cassiterite liberation. However, this result should be considered carefully since the feed grade of the sample from the conventional pathway was lower than the one of the EPF pre-treated sample (1.21% vs 1.71% respectively). Table 6
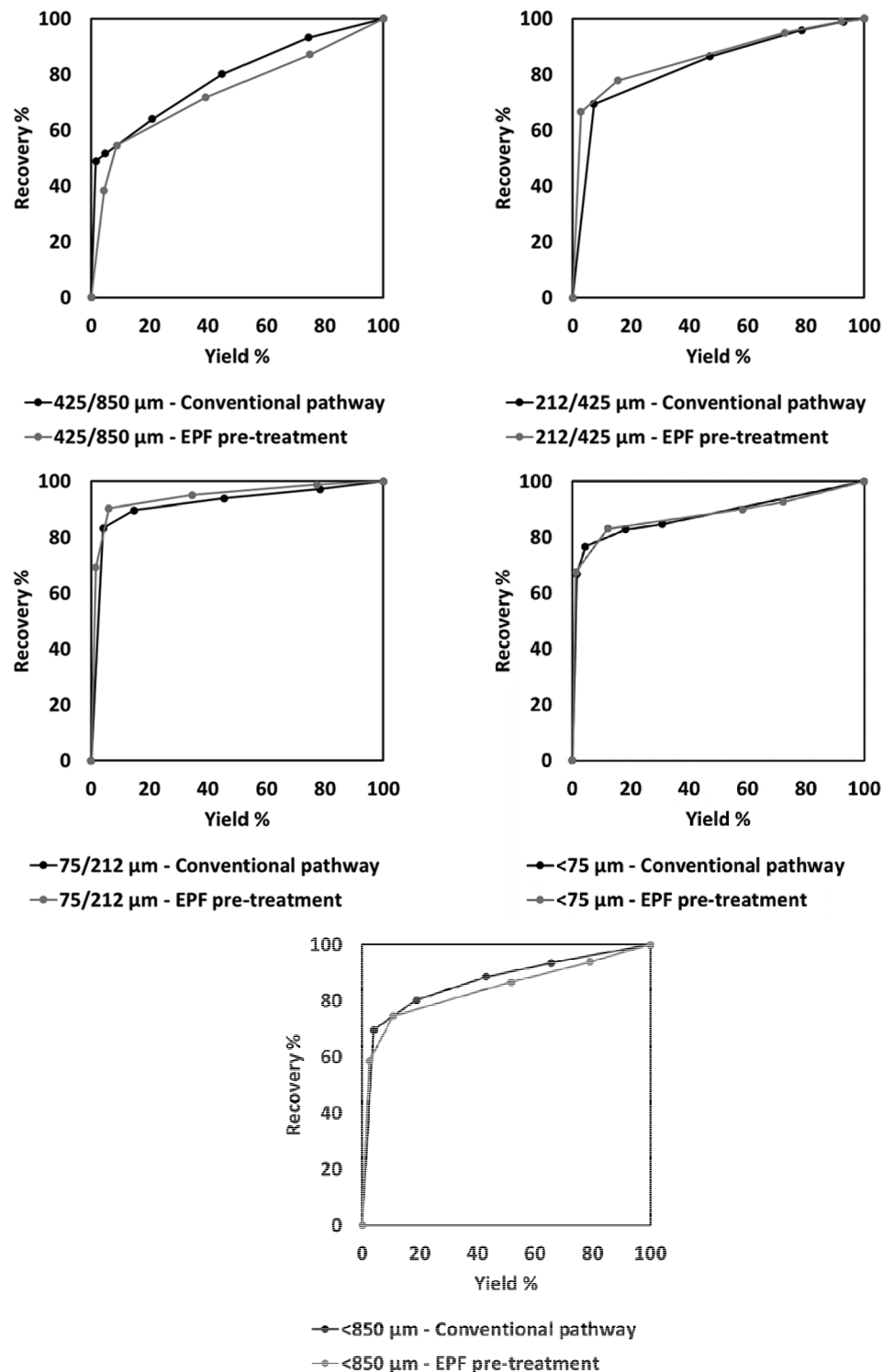
Fig. 12. Mayer diagram comparison of separation efficiency of the EPF Test 1 and of the conventional pathway.

and Fig. 12 also show that the tailings and the low-grade middlings still contained a high quantity of cassiterite, resulting in losses of about 20–30%, which indicates that cassiterite is not well liberated in both samples.

– In the size fractions 212/425 μm and 75/212 μm, a great increase of the concentrate grade was obtained with the Sn grade going from 13.89% to 31.30% for the size fraction 212/425 μm and from 30.51% to 73.30% for the size fraction 75/212 μm, but with a lower Sn recovery. This suggest that with a higher quantity of material

collected in the concentrate (higher mass-pull) the concentrate grade will decrease. The amount of losses in the tailings and low-grade middling indicates that gangue minerals are already liberated in this size range.

– In the size fraction < 75 μm, the cassiterite may be better liberated in the EPF pre-treated sample. The concentrates of both EPF and conventionally crushed samples showed a similar metal recovery (about 67%), however the EPF sample shows a higher Sn grade (67% against 50%) and lower mass-pull (1.15% against 1.50%). The

losses in tailings and low-grade middlings increased in the finest size fraction. This is not due to lack of liberation but to technical issues related to the Mozley table, in which very fine cassiterite particles can be indiscriminately dragged to the tailings by the aqua flow phenomenon (Gupta and Yan, 2016).

Weighing the results of all size fractions by the %mass of each size fraction, it was possible to calculate the performance of this gravity separation system in the whole sample (Table 6 and Fig. 12). Similar behaviors were observed in EPF and conventionally crushed samples, as shown in the Mayer diagrams (Fig. 12). A concentrate with a higher Sn grade was obtained when an EPF pre-treatment was applied but under lower recoveries. These results show that in this case there was no improvement in the gravity separation of cassiterite when including an EPF treatment in the comminution circuit.

The Mozley table tests were performed with the objective to obtain a first approach regarding the advantages of EPF pre-treatment in the further upgrading stages. Since no marked improvement was obtained, no upscaling tests were performed.

5. Conclusions

Electric Pulse Fragmentation (EPF) treatment is a novel method for ore fragmentation that has been shown to be able to either induce a dense fracture network within a material, thereby weakening it, or preferentially fragment parts of a material with higher metal contents deporting the metal-bearing minerals to a finer size fraction than waste rock. As part of a wider work to exploit low-grade European ore deposits, a cassiterite ore underwent EPF treatment to determine whether it could be weakened or concentrated to improve the economics of tin beneficiation for the mine. EPF was performed at pilot-scale to better simulate industrial processing conditions, and to have the opportunity to investigate the influence of this treatment on the downstream concentration processes. Two approaches for the implementation of the EPF treatment were investigated. The first approach consisted in using the EPF treatment for pre-concentration while in the second approach the EPF technology was primarily used for crushing.

The Bond rod mill work index performed on the EPF treated materials showed a reduction in energy needed to crush the material, while the Bond ball mill work index remained quite stable and an increase in abrasivity was observed. This is likely due to the deportment of some liberated minerals into a size fraction too small for the test, meaning test material possibly contained more resistant monomineralic particles such as quartz. For a better understanding of these results and confirmation of the hypothesis, additional tests should be performed and interpreted using liberation data.

Exploratory concentration tests performed with a Mozley Laboratory Separator showed that while EPF pre-treatment can lead to a higher concentrate grade, there is no conclusive evidence that EPF treatment could have a positive effect on the final Sn recovery. However, EPF operating conditions used were based on previous lab-scale testwork and were not optimized for a pilot-scale treatment of the ore. From these results, it is difficult to conclude the influence of the EPF treatment on the performances of the concentration processes. Further testwork would then be required to optimize the EPF process for this material, to identify and quantify the effects of an EPF treatment on subsequent concentration steps and to optimize the performances of the concentration processes.

Declaration of Competing Interest

The authors declare that they have no known competing financial interests or personal relationships that could have appeared to influence the work reported in this paper.

References

Andres, U., Jirestig, J., Timoshkin, I., 1999. Liberation of minerals by high-voltage electrical pulses. Powder Technol. 104, 37–49. https://doi.org/10.1016/S0032-5910(99)00024-8.

Angadi, S.I., Sreenivas, T., Jeon, H.-S., Baek, S.-H., Mishra, B.K., 2015. A review of cassiterite beneficiation fundamentals and plant practices. Miner. Eng. 70, 178–200. https://doi.org/10.1016/j.mineng.2014.09.009.

Bearman, R.A., 2013. Step change in the context of comminution. Miner. Eng. 43–44, 2–11.

Bru, K., Touzé, S., Auger, P., Dobrusky, S., Tierrie, J., Parvaz, D.B., 2018. Investigation of lab and pilot scale electric-pulse fragmentation systems for the recycling of ultra-high performance fibre-reinforced concrete. Miner. Eng. 128, 187–194. https://doi.org/10.1016/j.mineng.2018.08.040.

Gupta, A., Yan, D., 2016. Chapter 16 Gravity Separation. Min. Process. Des. Oper. 563–628.

Heinig, T., Bachmann, K., Tolosana-Delgado, R., van den Boogaart, K. G., Gutzmer, J. 2015. Monitoring gravitational and particle shape settling effects on MLA sample preparation. In: 17th Annual Conference of the International Association for Mathematical Geosciences, September 5-13 2015, Freiberg, Germany.

ITA (International Tin Association). 2013. Tin for Tomorrow. Contributing to Global Sustainable Development.

Kamali, A., Fray, D.J., 2011. Tin-based materials as advanced anode materials for lithium ion batteries: A review. Rev. Adv. Mater. Sci. 27, 14–24.

Kern, M., Kästner, J., Tolosana-Delgado, R., Jeske, T., Gutzmer, J., 2018. The inherent link between ore formation and geometallurgy as documented by complex tin mineralization at the Hämmerlein deposit (Erzgebirge, Germany). Miner. Deposita 54, 683–698. https://doi.org/10.1007/s00126-018-0832-2.

Moncrieff, A.G., Lewis, P.J., 1977. Treatment of Tin Ores. Trans. Inst. Min. Metall. 86, A56–A60.

Parvaz, D.B., Weh, A., von der Weid, F., 2019. Continuous electric pulse fragmentation of incinerator bottom ash: two years of industrial operation. MEI conference: Physical Separation, June 13-14 2019, Falmouth, UK.

Schuppan, W., Hiller, A., 2012. Die Komplexlagerstätten Tellerhäuser und Hämmerlein. Bergbaumonographie. Bergbau in Sachsen (Band 17). Freiberg: Sächsisches Landesamt für Umwelt und Geologie, Sächsisches Oberbergamt.

Shi, F., Zuo, W., Manlapig, E., 2013. Characterisation of pre-weakening effect on ores by high voltage electrical pulses based on single-particle tests. Miner. Eng. 50–51, 69–76. https://doi.org/10.1016/j.mineng.2013.06.017.

Shi, F., Zuo, W., Manlapig, E., 2015. Pre-concentration of copper ores by high voltage pulses. Part 2: Opportunities and challenges. Miner. Eng. 79, 315–323. https://doi.org/10.1016/j.mineng.2015.01.014.

Sultana, I., Ramireddy, T., Rahman, M.M., Chen, Y., Glushenkov, A.M., 2016. Tin-based composite anodes for potassium-ion batteries. Chem. Commun. 52, 9279–9282. https://doi.org/10.1039/C6CC03649J.

Tschugg, J., Öfner, W., Flachberger, H., 2017. Comparative laboratory studies of conventional and electrodynamic fragmentation of an industrial mineral. BHM Berg-Huettenmaenn. Monatsh. 162, 319–325. https://doi.org/10.1007/s00501-017-0638-z.

van der Wielen, K.P., Pascoe, R., Weh, A., Wall, F., Rollinson, G., 2013. The influence of equipment settings and rock properties on high voltage breakage. Miner. Eng. 46, 100–111. https://doi.org/10.1016/j.mineng.2013.02.008.

Wang, E., Shi, F., Manlapig, E., 2011. Pre-weakening of mineral ores by high voltage pulses. Miner. Eng. 24, 455–462. https://doi.org/10.1016/j.mineng.2010.12.011.

Wang, E., Shi, F., Manlapig, E., 2012. Mineral liberation by high voltage pulses and conventional comminution with same specific energy levels. Miner. Eng. 27, 28–36. https://doi.org/10.1016/j.mineng.2011.12.005.

Zuo, W., Shi, F., Manlapig, E., 2015. Pre-concentration of copper ores by high voltage pulses. Part 1: Principle and major findings. Miner. Eng. 79, 306–314. https://doi.org/10.1016/j.mineng.2015.03.022.

Zuo, W., 2015. A study of the applications and modelling of high voltage pulse comminution for mineral ores, Thesis Sustainable Minerals Institute, University of Queensland.